

Robust Reconstruction of Grid Frequency in Disturbed Converter-Based Power Systems by Takagi-Sugeno Fuzzy Approach

Nico Goldschmidt¹, Horst Schulte¹, Ignacio Glenney Crende²

¹ University of Applied Sciences (HTW) Berlin,
Faculty 1: School of Engineering - Energy and Information,
Wilhelminenhofstr. 75A, 12459 Berlin, Germany,
Email: schulte@htw-berlin.de

² Universitat Politècnica de Catalunya
Department d'Enginyeria Elèctrica (CITCEA-UPC)
UPC. Av. Diagonal 647, Pl. 2, Barcelona, 08028, Spain
Email: ignacio.glenney@upc.edu

Summary

This study investigates the conversion of the proposed phase-locked loop design into the Takagi-Sugeno fuzzy model approach. Here, the Takagi-Sugeno fuzzy model is used to describe the nonlinear dynamics of the PLL system through fuzzy rules that summarize locally linear submodels. By applying the fuzzy model, the control performance of the PLL system can be further improved, and adaptability to different operating conditions can be enhanced. The work shows how state feedback and pole placement can be integrated into the Takagi-Sugeno fuzzy framework, enabling robust and precise frequency estimation under disturbed conditions. Simulations illustrate the effectiveness of the combined approach and highlight its potential for application in power systems.

1 Introduction

The continuous expansion of renewable energy in power grids aims for 100% renewable energy production, necessitating their integration as active control units for grid stabilization. Reducing conventional energy producers introduces more disturbances and harmonics, resulting in higher frequency and voltage variations. Precise detection of fundamental symmetrical components is crucial for the reliable operation of inverter-based renewable energy sources, even in disrupted areas.

This work focuses on exact frequency reconstruction in converter-based three-phase grids. A key challenge is the reliable reconstruction of heavily loaded systems due to harmonics and other disturbances. Unlike traditional phase-locked loops that filter out disturbances, the method by [1] employs a recursive estimation process. First, it reconstructs the fundamental oscillation from the disturbed signal, then it reconstructs the grid frequency using a model-based phase-locked loop (PLL). This method has proven effective even in highly disturbed grids. Previous work by [2] introduced a linear model-based I-extended state feedback, achieving fast and precise results, particularly in 50Hz grids, and effective performance with larger frequency deviations. The community's curiosity about future systems operating at non-fixed frequencies led to exploring an extension using nonlinear control methods.

The extension in this paper relies on the recursive estimation method for fundamental oscillation reconstruction, serving as a base signal for frequency reconstruction. For final frequency reconstruction and deviating operating frequencies, a Takagi-Sugeno Fuzzy model [3] is used. This model simplifies the nonlinear dynamics of the PLL into local linear submodels, achieving the desired operating range. The previous model-based state controllers and pole assignment methods are combined with the Takagi-Sugeno approach using Linear Matrix Inequalities (LMI).

The work is structured as follows: Section 2 reviews the modeling from previous work, setting the stage for the extension in Section 3. Stability is ensured using the Takagi-Sugeno method. Section 4 presents simulation results, followed by the conclusion in Section 5.

2 Modeling

In the paper [2] published in 2020, the systematic design of an I-extended state controller for a phase-locked loop was presented, which reconstructs the grid angle based on an estimated fundamental oscillation of a disturbed grid using a Least Mean Square estimator based on [1]. The formal basis of PLL modeling is provided by the synchronous voltage reference frame in d - q coordinates. The corresponding coordinators $\mathbf{v}_{dq} = (v_d \ v_q)^T$ are calculated from the symmetric components of the three phase system $\mathbf{v}_{abc} = (v_a \ v_b \ v_c)^T$ by the Clark and Park transformation

$$\begin{pmatrix} v_d \\ v_q \end{pmatrix} = \underbrace{\frac{2}{3} \begin{pmatrix} \cos(\hat{\varphi}) & \cos(\hat{\varphi} - \frac{2}{3}\pi) & \cos(\hat{\varphi} + \frac{2}{3}\pi) \\ -\sin(\hat{\varphi}) & -\sin(\hat{\varphi} - \frac{2}{3}\pi) & -\sin(\hat{\varphi} + \frac{2}{3}\pi) \end{pmatrix}}_{\mathbf{T}_{dq}(\hat{\varphi})} \begin{pmatrix} v_a \\ v_b \\ v_c \end{pmatrix}, \quad (1)$$

where $\hat{\varphi}$ denotes the estimated phase angle. It should be noted that a synchronous coordinate system can be formed with the Clark and Park transformation (1) if the three-phase system is symmetric. Thus (1) can be applied to a unbalanced system by transforming $\mathbf{v}_{abc} = (v_a \ v_b \ v_c)^T$ in symmetric components with

$$\mathbf{v}_{abc} = \mathbf{v}_{abc}^+ + \mathbf{v}_{abc}^- + \mathbf{v}_{abc}^0 \quad (2)$$

with the positive sequence components \mathbf{v}_x^+ , negative sequence components \mathbf{v}_x^- , and zero sequence components \mathbf{v}_x^0 . Note that the zero components are not taken into account because the park transformation yields a zero vector. By substituting follows with (1) and the addition theorem

$$\begin{aligned} v_d &= \underbrace{-V^+ \sin(\Delta\hat{\varphi}^+)}_{v_d^+} + \underbrace{V^- \sin(\Delta\hat{\varphi}^+ - \varphi_n)}_{v_d^-} \\ v_q &= \underbrace{V^+ \cos(\Delta\hat{\varphi}^+)}_{v_q^+} - \underbrace{V^- \cos(\Delta\hat{\varphi}^+ - \varphi_n)}_{v_q^-}, \end{aligned} \quad (3)$$

where $\Delta\hat{\varphi}^+$ denotes the difference between of the reconstructed and true phase angle

$$\Delta\hat{\varphi}^+ = \varphi^+ - \hat{\varphi} \quad . \quad (4)$$

The derivation of (3) leads to

$$\begin{aligned} \dot{v}_d^+ &= - \Delta\hat{\omega}^+ V^+ \cos(\Delta\hat{\varphi}^+) \\ \dot{v}_q^+ &= - \Delta\hat{\omega}^+ V^+ \sin(\Delta\hat{\varphi}^+) \\ \dot{v}_d^- &= (\Delta\hat{\omega}^+ - \omega_n) V^- \cos(\Delta\hat{\varphi}^+ - \varphi_n) \\ \dot{v}_q^- &= (\Delta\hat{\omega}^+ - \omega_n) V^- \sin(\Delta\hat{\varphi}^+ - \varphi_n) \end{aligned} \quad (5)$$

with

$$\Delta\hat{\omega}^+ = \Delta\hat{\varphi}^+ , \quad \omega_n = \dot{\varphi}_n >> 0 \quad . \quad (6)$$

The differential equation system is simplified by inserting (3) into (5). In summary, this results in

$$\begin{pmatrix} \dot{v}_d^+ \\ \dot{v}_q^+ \\ \dot{v}_d^- \\ \dot{v}_q^- \end{pmatrix} = \begin{pmatrix} -\Delta\hat{\omega}^+ v_q^+ \\ \Delta\hat{\omega}^+ v_d^+ \\ -\Delta\hat{\omega}^+ v_q^- \\ \Delta\hat{\omega}^+ v_d^- \end{pmatrix} . \quad (7)$$

For the model-oriented control design it is necessary to transform (7) in the state-space form:

$$\dot{\mathbf{x}} = \mathbf{f}(\mathbf{x}, u) = \begin{pmatrix} 0 & -u & 0 & 0 \\ u & 0 & 0 & 0 \\ 0 & 0 & 0 & -u \\ 0 & 0 & u & 0 \end{pmatrix} \mathbf{x} = \mathbf{A}(u) \mathbf{x} \quad (8)$$

with the state vector

$$\mathbf{x} = (\mathbf{x}^+, \mathbf{x}^-)^T = (v_d^+, v_q^+, v_d^-, v_q^-)^T , \quad (9)$$

the output vector \mathbf{y} and scalar valued input u , i.e.

$$\mathbf{y} = \mathbf{x}, \quad u = \Delta \hat{\omega}^+ . \quad (10)$$

It is interesting to note that the deduced nonlinear state-space model (8) has no affine input u but appears as a variable parameter in the system matrix $\mathbf{A}(u)$.

2.1 State Space Feedback Design for Setpoint Sequences with Pole Specification

Based on the Taylor-linearized model in (8) a systematic LMI-based design according to [4], [5], [6] is presented for further use in the entire PLL synthesis. In contrast to classical PI controller design the approach enables a pole placement in a desired region in the complex plane by LMI-constraints. For stationary exactness the system will be extended to a setpoint control for $\mathbf{y}_{ref} \neq \mathbf{0}$. In order to be able to guarantee the stability of the closed loop, the integrator eigenvalues must be controllable. According to the criterion of Hautus, the r integral eigenvalues $\lambda = 0$ can be controlled, if and only if the condition

$$\text{Rank} \left(\begin{array}{cc|c} \mathbf{A}_c & \mathbf{0} & \mathbf{b}_c \\ \mathbf{c}_c^T & 0 & d_c \end{array} \right) = n + r \quad (11)$$

is fulfilled. For the estimation of the actual angular frequency value with the synchronous reference frame approach the exact regulation of the positive q component to ZERO is necessary, so the output matrix \mathbf{c}_c is defined by

$$\mathbf{c}_c^T = \begin{pmatrix} 0 & 1 & 0 & 0 \end{pmatrix} . \quad (12)$$

Taking into account the output matrix \mathbf{c}_c , we get the extended system and input matrix

$$\tilde{\mathbf{A}}_c = \begin{pmatrix} \mathbf{A}_c & \mathbf{0} \\ -\mathbf{c}_c^T & 0 \end{pmatrix} \in \mathbb{R}^{(n+1) \times (n+1)}, \quad \tilde{\mathbf{b}}_c = \begin{pmatrix} \mathbf{b} \\ 0 \end{pmatrix} \in \mathbb{R}^{(n+1) \times m} . \quad (13)$$

The setpoint control law can then be specified for the extended system with the input

$$\Delta \tilde{u} = - \begin{pmatrix} \mathbf{k}_x & -k_I \end{pmatrix} \quad (14)$$

and

$$\Delta r = \int_0^t \Delta e d\tau, \quad \Delta e = \Delta y_{ref} - \mathbf{c}_c^T \Delta \mathbf{x} \quad (15)$$

as follows

$$\Delta \tilde{u} = -\mathbf{k}_x^T \Delta \mathbf{x} + k_I \int \Delta \quad (16)$$

For the sake of clarity, previous results are summarized in Fig. 1. The block

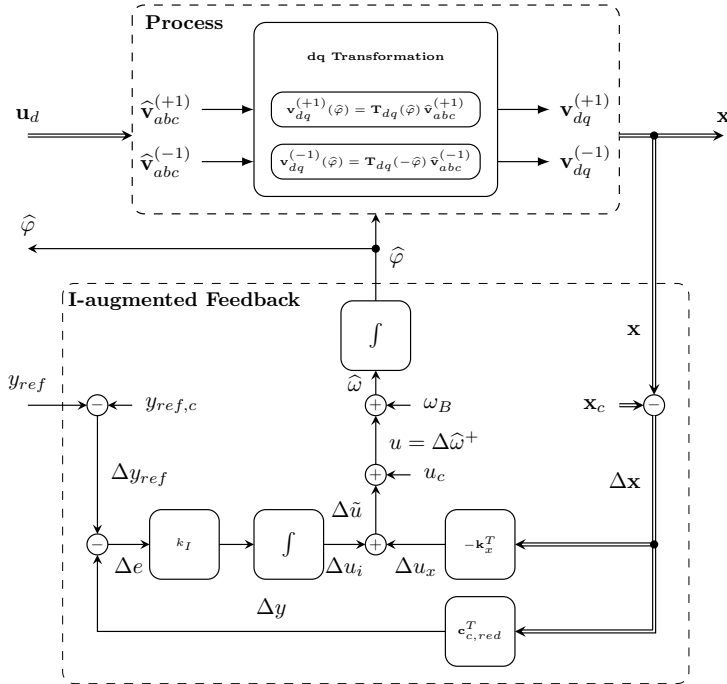


Figure 1: Block diagram of the I-augmented feedback control

diagram illustrates the I-augmented state feedback structure including the transformation of a three phase system into a synchronous reference frame for positive and negative sequences. Based on the extended uncertain system of (8)

$$\Delta \tilde{\mathbf{x}} = \tilde{\mathbf{A}}_c \Delta \tilde{\mathbf{x}} + \tilde{\mathbf{b}}_c \Delta \tilde{u} \quad (17)$$

with the equilibrium point

$$\mathbf{x}_c = [1, 0, 0, 0]^T, \quad u_c = 0, \quad (18)$$

\mathbf{A}_c as the system matrix and \mathbf{b}_c as the input vector, the objective is to find a state variable feedback

$$\Delta \tilde{u} = -\tilde{\mathbf{k}}^T \Delta \tilde{\mathbf{x}} \quad (19)$$

such that the closed-loop eigenvalues of $(\tilde{\mathbf{A}} - \tilde{\mathbf{b}}\tilde{\mathbf{k}}^T)$ are in $S(\alpha_{min}, \alpha_{max})$. The so-defined pole region $S(\alpha_{min}, \alpha_{max})$ is shown in Fig. 2. The constraint pre-

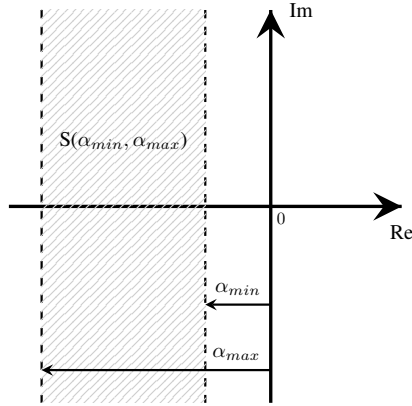


Figure 2: Pole region $S(\alpha_{min}, \alpha_{max})$

defined region of closed loop eigenvalues $S(\alpha_{min}, \alpha_{max})$ guarantees a desired performance specified by an maximum overshoot, the frequency range of the damped oscillations, rise time, and settling time as shown in [4]. However, it is assumed that there is a feasible solution to the LMI condition (22). The system

(17) controlled by state feedback (19) is exponentially stable in respect to the defined region $S(\alpha_{min}, \alpha_{max})$ if there exists a Lyapunov function

$$\mathbf{V}(\Delta\tilde{\mathbf{x}}) = \Delta\tilde{\mathbf{x}}^T \mathbf{P} \Delta\tilde{\mathbf{x}}, \mathbf{P} > 0 \quad (20)$$

with $\mathbf{P} = \mathbf{P}^T \in \mathbb{R}^{n+r \times n+r}$ and $\mathbf{X} = \mathbf{P}^{-1}$ that fulfills with respect to

$$\mathbf{P}\mathbf{A}_c^T + \mathbf{A}_c\mathbf{P} < \mathbf{b}_c\mathbf{m} + \mathbf{m}^T\mathbf{b}_c^T, \quad (21)$$

where and $\mathbf{m} \in \mathbb{R}^{1 \times n}$. The LMI stability are given by

$$\begin{aligned} -2\alpha_{max}\mathbf{X} &< \tilde{\mathbf{A}}_c\mathbf{X} + \mathbf{X}\tilde{\mathbf{A}}_c^T - \tilde{\mathbf{b}}_c\mathbf{m} - \mathbf{m}^T\tilde{\mathbf{b}}_c^T < -2\alpha_{min}\mathbf{X} \\ \begin{pmatrix} -r\mathbf{P} & \mathbf{A}\mathbf{P} - \mathbf{b}\mathbf{m} \\ \mathbf{P}\mathbf{A}^T - \mathbf{m}^T\mathbf{b}^T & -r\mathbf{P} \end{pmatrix} &< 0 \\ (\mathbf{E} \otimes \mathbf{A})\mathbf{P} + \mathbf{P}(\mathbf{E} \otimes \mathbf{A})^T - (\mathbf{E} \otimes \mathbf{b})\mathbf{m} - \mathbf{m}^T(\mathbf{E} \otimes \mathbf{b})^T &< 0 \end{aligned} \quad (22)$$

with

$$\mathbf{E} = \begin{pmatrix} \sin \theta & \cos \theta \\ -\cos \theta & \sin \theta \end{pmatrix}, \quad (23)$$

with $\alpha_{max} > \alpha_{min} > 0$, where $\mathbf{m} \in \mathbb{R}^{1 \times n+r}$. As described in [4] and [5]

$$\begin{pmatrix} \sin \theta (\mathbf{A}\mathbf{X} + \mathbf{X}\mathbf{A}^T - \mathbf{M}^T\mathbf{B}^T - \mathbf{B}\mathbf{M}) & \cos \theta (\mathbf{A}\mathbf{X} - \mathbf{X}\mathbf{A}^T + \mathbf{M}^T\mathbf{B}^T - \mathbf{B}\mathbf{M}) \\ \cos \theta (-\mathbf{A}\mathbf{X} + \mathbf{X}\mathbf{A}^T - \mathbf{M}^T\mathbf{B}^T + \mathbf{B}\mathbf{M}) & \sin \theta (\mathbf{A}\mathbf{X} + \mathbf{X}\mathbf{A}^T - \mathbf{M}^T\mathbf{B}^T - \mathbf{B}\mathbf{M}) \end{pmatrix} < 0 \quad (24)$$

this results in the state feedback matrix

$$\tilde{\mathbf{k}}^T = \mathbf{m}\mathbf{X}^{-1} \quad (25)$$

for (19).

3 Takagi-Sugeno Control with Prefilter Design

In this work, the fuzzy approximation of the nonlinear state-space model is formulated using the Takagi-Sugeno (TS) model structure. Originally introduced

in the context of fuzzy systems by [3], TS models are weighted combinations of linear or affine sub-models. These models can be derived either from input-output data using system identification techniques, as presented by [3], [7] and [8]. The general Takagi-Sugeno (TS) structure of a state-space model with so-called affine remainder terms is of the form:

$$\begin{aligned}\dot{\mathbf{x}} &= \sum_{i=1}^{N_r} h_i(\mathbf{z})(\mathbf{A}_i\mathbf{x} + \mathbf{B}_i\mathbf{u} + \mathbf{a}_i) \\ \mathbf{y} &= \sum_{i=1}^{N_r} h_i(\mathbf{z})(\mathbf{C}_i\mathbf{x} + \mathbf{D}_i\mathbf{u} + \mathbf{c}_i)\end{aligned}\quad (26)$$

where $\mathbf{z} \in \mathbb{R}^{N_l}$ denotes the vector of premise variables, $\mathbf{x} \in \mathbb{R}^n$ is the vector of system states, $\mathbf{u} \in \mathbb{R}^m$ is the input vector, $\mathbf{y} \in \mathbb{R}^p$ is the vector of outputs. The matrices \mathbf{A}_i , \mathbf{B}_i , \mathbf{C}_i , and \mathbf{D}_i , and the affine vectors \mathbf{a}_i and \mathbf{c}_i , are of appropriate dimensions. The membership functions h_i fulfill the following conditions:

$$\begin{aligned}\sum_{i=1}^{N_r} h_i(\mathbf{z}) &= 1, \quad \text{for } i = 1, \dots, N_r, \\ h_i(\mathbf{z}) &\geq 0, \quad i = 1, \dots, N_r,\end{aligned}\quad (27)$$

where the above is known as the convex sum condition. The Takagi-Sugeno fuzzy approximation of the nonlinear state-space model (8) is now determined. First, the variables that govern the nonlinearities must be identified, as the scheduling vector should consist of these variables. This involves deciding on \mathbf{z} as a selection of inputs, states, outputs, and external measurements. In this case, the scheduling vector is chosen based on the input

$$\mathbf{z} = \mathbf{u} = \Delta\hat{\omega}^+. \quad (28)$$

With frequency deviation $\Delta\hat{\omega}^+$ the frequencies f_{\min} , f_{\max} , and f_{ref} are defined as follows:

$$f_{\min} \leq f_{\text{ref}} \leq f_{\max} \quad \text{where} \quad 45\text{Hz} \leq 50\text{Hz} \leq 55\text{Hz} . \quad (29)$$

The vector of equilibrium points $u_{c,i}$ for $i = 1, \dots, N_r$ is defined as follows:

$$\mathbf{u}_c = 2\pi(-5.0; -4.8; -4.6; \dots; u_{c,i}; \dots; 4.6; 4.8; 5.0)^T, \quad (30)$$

where $N_r = 51$ has been chosen as a good compromise between accuracy and performance. A Takagi-Sugeno fuzzy controller with prefilter in the following compact form is proposed

$$\Delta u = \mathbf{h}(z) \mathbf{V} \Delta \mathbf{x}_{\text{ref}} - \mathbf{h}(z) \mathbf{K} \Delta \mathbf{x}, \quad (31)$$

where the prefilter matrix is given

$$\mathbf{V} = \begin{pmatrix} v_{1,1} & v_{2,1} & v_{3,1} & v_{4,1} \\ \vdots & \vdots & \vdots & \vdots \\ v_{1,i} & v_{2,i} & v_{3,i} & v_{4,i} \\ \vdots & \vdots & \vdots & \vdots \\ v_{1,N_r} & v_{2,N_r} & v_{3,N_r} & v_{4,N_r} \end{pmatrix}$$

and the feedback gains are arranged as

$$\mathbf{K} = \begin{pmatrix} k_{1,1} & k_{2,1} & k_{3,1} & k_{4,1} \\ \vdots & \vdots & \vdots & \vdots \\ k_{1,i} & k_{2,i} & k_{3,i} & k_{4,i} \\ \vdots & \vdots & \vdots & \vdots \\ k_{1,N_r} & k_{2,N_r} & k_{3,N_r} & k_{4,N_r} \end{pmatrix}.$$

In combination with the row vector of all membership functions

$$\mathbf{h}(z) = (h_1(z) \ h_2(z) \ \dots \ h_{N_r-1}(z) \ h_{N_r}(z)) \quad (32)$$

the formula (31) represents the compact matrix form of a Takagi-Sugeno control law with prefilter. To calculate the absolute output of (31), the values of the equilibrium points must still be taken into account by

$$u = \mathbf{h}(z) \mathbf{u}_c + \Delta u. \quad (33)$$

Obtaining the estimated phase for the positive sequence θ^+ after $\Delta \hat{\omega}^+ = u$ has been determined requires the equilibrium frequencies. The reconstructed

frequency \hat{f} is as follows:

$$\hat{f} = \mathbf{h}(z)\mathbf{f}_c^T - \Delta\hat{\omega}^+ \quad (34)$$

This reconstructed frequency \hat{f} is then passed through an integrator in order to obtain the estimated phase θ^+ .

4 Results and Discussion

In this paper, three primary events are used to compare the performance of the proposed TS prefilter PLL with an I-augmented PLL and a linear (static gain) prefilter PLL. The first simulated event is a phase-to-phase short circuit lasting 0.5 seconds. This event is evaluated in three different scenarios:

- Clean (Clean): No harmonics or measurement disturbances are present
- Low Harmonics (LH): Includes measurement disturbances
- High Harmonics (HH): Includes significant measurement disturbances

While the short circuit last for 0.5 seconds, the full simulation runs for 1 second. The second simulated event is a frequency variation (FreqVar) lasting 30 seconds. As in the short circuit, the three scenarios (clean, LH, and HH) are also considered here. The Table 1 shoes the key results of these simulations, including additional details about the various test conditions and scenarios.

Event	Short circuit			Freq. Variation		
	Clean	LH	HH	Clean	LH	HH
Duration (s)	1	1	1	30	30	30
Disturbance	Yes	Yes	Yes	Yes	Yes	Yes
5th Harmonic [%]	0.00	3.0	30.0	0.00	3.0	30.0
7th Harmonic [%]	0.0	1.5	15.0	0.0	1.5	15.0
V_d^+ SS Error [p.u.]	$7.4 \cdot 10^{-4}$	$7.4 \cdot 10^{-4}$	$7.4 \cdot 10^{-4}$	$4 \cdot 10^{-2}$	$4 \cdot 10^{-2}$	$4 \cdot 10^{-2}$
Settling Time [s]	0.038	0.038	0.038	-	-	-

Table 1: Key indicators with details about every simulation run

4.1 Disturbances and Harmonics

The disturbance is introduced as random noise in the measurements. Figure 3(a) displays the three-phase voltage for the clean scenario, where no harmonics or measurement disturbances are present. In contrast, the effects of disturbance on the source voltage are illustrated in Figure 3(b).

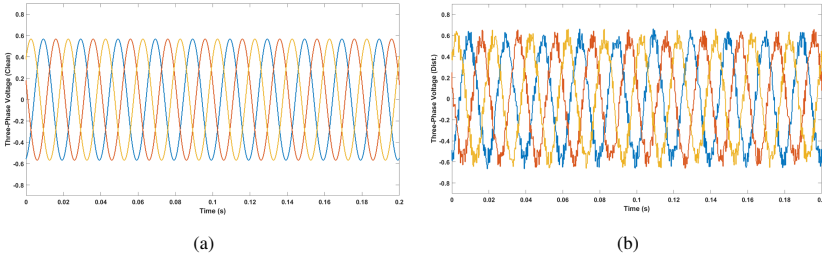


Figure 3: 3ph voltage at the source without (a) and with (b) measurement disturbance

Figures 4(a) and (b) show the disturbed 3ph system, which is intended to affect the PLL's ability to track the system's phase. No separate scenarios are considered solely for the disturbance. It is shown that the impact of the disturbance is negligible and it is included in the Low Harmonics and High Harmonics scenarios.

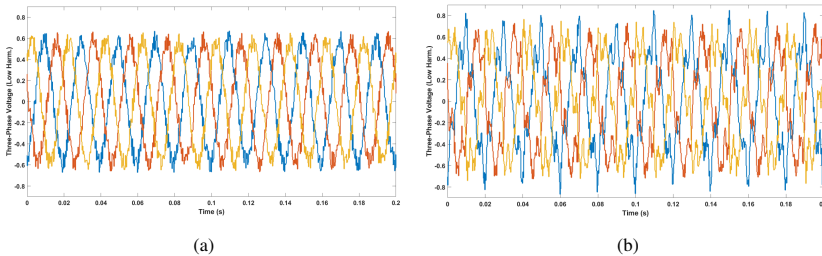


Figure 4: Three phase voltage at the source for the Low Harmonics (a) and for the High Harmonics (b) scenario

4.2 Short Circuit scenario

Figure 5(a), 5(b) and Figure 7 illustrate the evolution of V_d^+ , V_q^+ , and Δf , respectively, throughout the entire short circuit simulation run under the High Harmonics scenario. In Figure 5, a voltage dip in V_d^+ , V_q^+ can be observed, which measures some p.u. (a certain percentage of the steady-state value) as a result of phase-to-phase short circuit.

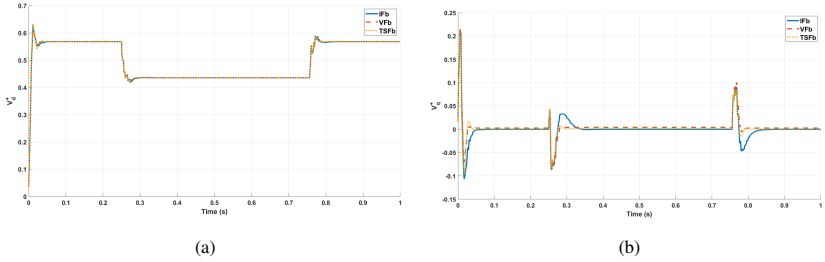


Figure 5: V_d^+ voltage (a) and V_q^+ voltage (b) for the short circuit High Harmonics scenario

The I-augmented PLL (IFB) requires more time to reach $V_q^+ = 0$ after the short circuit event; however, it is the only method that achieves this without any steady-state error. In contrast, the Static Prefilter (VFb) and the Takagi-Sugeno Static Prefilter (TSFb) exhibit steady-state errors of value and value p.u., respectively. This can be observed in Figure 5(b) below.

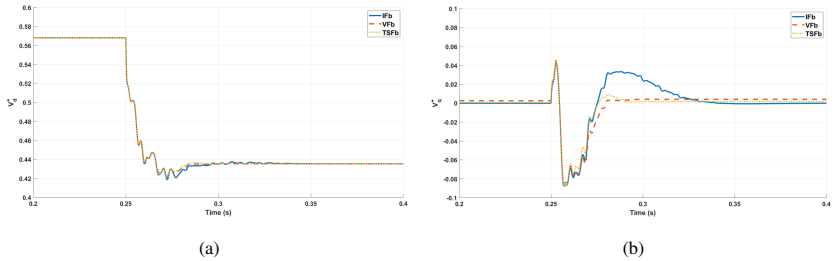


Figure 6: Detail of V_d^+ voltage (a) and V_q^+ voltage (b) for the short circuit High Harmonics scenario

To illustrate the transition that systems undergo during the short-circuit event, the Figures 6(a) and 6(b) detail the transition period. The longer settling time of the I-augmented PLL (IFB) is more clearly visible in Figure 6(a).

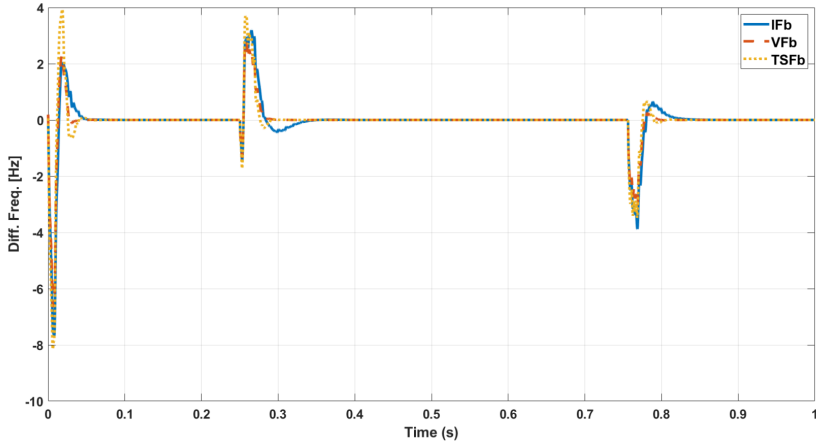


Figure 7: Δf for the short circuit High Harmonics scenario

The overshoot and longer settling times of the I-augmented PLL (IFB) in V_q^+ can be observed in Figure 6(b), alongside the steady-state errors of the Static Prefilter (VFb) and the Takagi-Sugeno Prefilter (TSFb). All three PLL systems successfully reach the nominal steady-state frequency of 50 Hz, as shown in Figure 7. The settling time required by each of the PLLs to reach the target steady-state value, as seen in Table 1, is graphically represented in Figures 8(a) and (b) below.

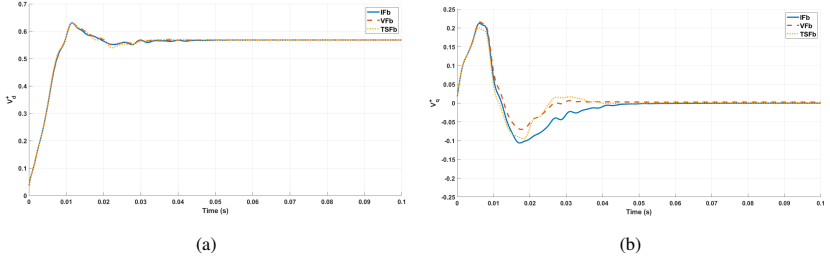


Figure 8: V_d^+ voltage (a) and V_q^+ voltage (b) in the initial transient for the short circuit High Harmonics scenario

4.3 Frequency Variation scenario

The evolution of the source frequency during the entire simulation run of frequency variation is shown in Figure 9(a). All three PLL systems are able to reach different target steady-state frequencies. However, as seen in Figure 9(b), the Static Prefilter (VFb) and Takagi-Sugeno (TSFb) PLL exhibit small steady-state errors ranging from 2 to -6 mHz.

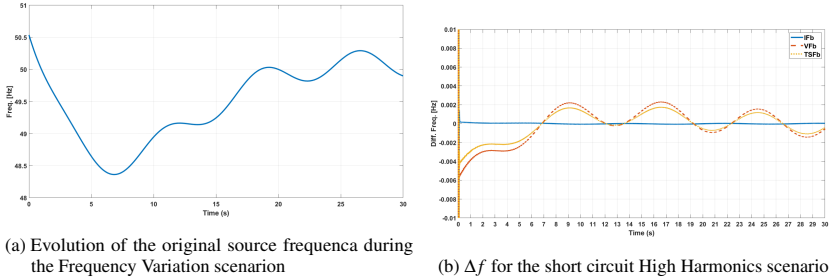


Figure 9: Frequency variation scenario

Figure 10(a) and (b) illustrate the evolution of V_d^+ and V_q^+ , respectively, throughout the simulation run of frequency variation for the high harmony scenario. A difference in the V_d^+ voltages among the three PLLs can be observed in Figure 10(a).

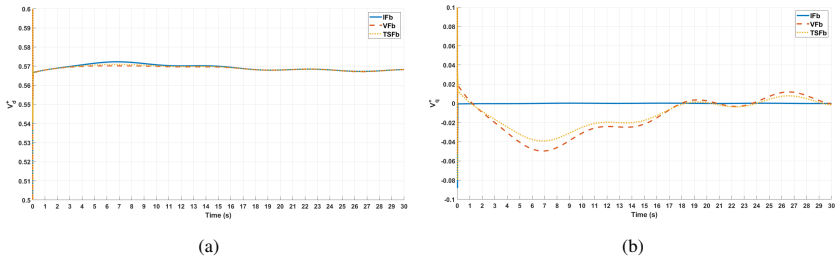


Figure 10: V_d^+ voltage (a) and V_q^+ voltage (b) for the short circuit High Harmonics scenario

The Static Prefilter (VFb) and the Takagi-Sugeno (TSFb) PLLs are unable to achieve $V_q^+ = 0$ when the frequency deviates from 50 Hz. This steady-state error is displayed in Figure 10(b).

5 Conclusion

Using an electrical modeling and the I-augmented and Standard Prefilter PLL environments developed by [2], simulations of short-circuits, load jumps, and frequency variation events under various disturbance and harmonic scenarios were conducted. Short-circuit and frequency variation simulation results are included in this paper to demonstrate the phase-tracking capabilities of the TS Static Prefilter. The Least Mean Squares filter used to reconstruct the main harmonic is crucial for the results obtained by the various PLLs studied in this work, but its development is beyond the scope of this paper.

References

- [1] X. Zhang, X. Cao, W. Wang, and C. Yun, Fault Ride-Through Study of Wind Turbines, *Journal of Power and Energy Engineering*, vol. 01, no. 05, pp. 25–29, 2013. [Online]. Available: <http://www.scirp.org/journal/doi.aspx?DOI=10.4236/jpee.2013.15004>

- [2] N. Goldschmidt and H. Schulte, Estimation of Grid Frequency in Disturbed Converter-Based Power Systems by PLL State Variable Feedback, In: Proceedings of IFAC World Congress 2020, Berlin, Germany, 2020.
- [3] T. Takagi and M. Sugeno, “Fuzzy Identification of Systems and Its Application to Modeling and Control,” *IEEE Transactions on Systems, Man, and Cybernetics*, vol. 15, no. 1, pp. 116–132, 1985.
- [4] M. Chilali and P. Gahinet, “H_{infty} design with pole placement constraints: An LMI approach,” *IEEE Transactions on Automatic Control*, vol. 41, no. 3, pp. 358–367, 1996.
- [5] D. Arzelier, J. Bernussou, and G. Garcia, “Pole assignment of linear uncertain systems in a sector via a Lyapunov-type approach,” *IEEE Transactions on Automatic Control*, vol. 38, no. 7, pp. 1128–1132, 1993.
- [6] S. Gutman and E. Jury, A general theory for matrix root-clustering in subregions of the complex plane, *IEEE Transactions on Automatic Control*, vol. 26, no. 4, pp. 853–863, Aug. 1981. [Online]. Available: <http://ieeexplore.ieee.org/document/1102764/>
- [7] M. Sugeno and G. T. Kang, “Structure Identification of Fuzzy Models,” *Fuzzy Sets and Systems*, vol. 28, pp. 15–33, 1988.
- [8] Z. Lendek, T. M. Guerra, R. Babuška, and B. de Schutter, *Stability Analysis and Nonlinear Observer Design Using Takagi-Sugeno Fuzzy Models*. Springer-Verlag Berlin Heidelberg, 2010.
- [9] K. Tanaka, T. Ikeda, and H. O. Wang, “Robust stabilization of a class of uncertain nonlinear systems via fuzzy control: quadratic stabilizability, H_{infty} control theory, and linear matrix inequalities,” *IEEE Transactions on Fuzzy Systems*, vol. 4, pp. 1–13, 1996.